

# Preclinical development of a humanized chimeric antigen receptor against B-cell maturation antigen for multiple myeloma



Lorena Perez-Amill,<sup>1</sup> Guillermo Suñe,<sup>1</sup> Asier Antoñana-Vildosola,<sup>1</sup> Maria Castella,<sup>1</sup> Amer Najjar,<sup>2</sup> Jaume Bonet,<sup>3</sup> Narcis Fernández-Fuentes,<sup>4</sup> Susana Inogés,<sup>5</sup> Ascensión López,<sup>5</sup> Clara Bueno,<sup>6</sup> Manel Juan,<sup>7</sup> Alvaro Urbano-Ispizua<sup>1,8,9</sup> and Beatriz Martín-Antonio<sup>1,8</sup>

<sup>1</sup>Department of Hematology, Hospital Clinic, IDIBAPS, Barcelona, Spain; <sup>2</sup>Department of Pediatrics - Research, The University of Texas M. D. Anderson Cancer Center, Houston, TX, USA; <sup>3</sup>Laboratory of Protein Design and Immunoengineering, École Polytechnique Fédérale de Lausanne, Lausanne, Switzerland; <sup>4</sup>Department of Biosciences, Faculty of Sciences and Technology, Universitat de Vic - Universitat Central de Catalunya, Vic, Spain; <sup>5</sup>Department of Hematology and Cell Therapy Area and Department of Immunology and Immunotherapy, Clinic University of Navarra, Navarra, Spain; <sup>6</sup>Josep Carreras Leukemia Research Institute and Cell Therapy Program of the School of Medicine, University of Barcelona, Barcelona, Spain; <sup>7</sup>Department of Immunotherapy, Hospital Clinic, IDIBAPS, Barcelona, Spain; <sup>8</sup>Josep Carreras Leukemia Research Institute, Barcelona, Spain and <sup>9</sup>Department of Hematology, University of Barcelona, Barcelona, Spain

Haematologica 2021  
Volume 106(1):173-184

## ABSTRACT

Multiple myeloma is a prevalent and incurable disease, despite the development of new and effective drugs. The recent development of chimeric antigen receptor (CAR)T cells has shown impressive results in the treatment of patients with relapsed or refractory hematologic B-cell malignancies. In recent years, B-cell maturation antigen (BCMA) has appeared as a promising antigen to target using a variety of immunotherapy treatments, including CART cells, for patients with multiple myeloma. To this end, we generated clinical-grade murine CART cells directed against BCMA, named ARI2m cells. Having demonstrated its efficacy, and in an attempt to avoid the immune rejection of CART cells by the patient, the single chain variable fragment was humanized, creating ARI2h cells. ARI2h cells showed comparable *in vitro* and *in vivo* efficacy to that of ARI2m cells, and superiority in cases of high tumor burden disease. In terms of inflammatory response, ARI2h cells produced less tumor necrosis factor- $\alpha$  and were associated with a milder *in vivo* toxicity profile. Large-scale expansion of both ARI2m and ARI2h cells was efficiently conducted following Good Manufacturing Practice guidelines, obtaining the target CART-cell dose required for treatment of multiple myeloma patients. Moreover, we demonstrated that soluble BCMA and BCMA released in vesicles both affect CAR-BCMA activity. In summary, this study sets the bases for the implementation of a clinical trial (EudraCT code: 2019-001472-11) to study the efficacy of ARI2h-cell treatment for patients with multiple myeloma.

## Introduction

Multiple myeloma (MM) remains an incurable hematologic malignancy responsible for 15-20% of all blood cancers<sup>1,2</sup> and new cases have been increasing, on average, by 0.8% each year over the past decade.<sup>3</sup> The natural history of MM is relapse until refractory disease without reaching a plateau of survival, with less than 10% of patients achieving sustained complete remission beyond 5-10 years after autologous stem-cell transplantation.<sup>4</sup> Moreover, patients are rarely cured after high-dose chemotherapy followed by autologous stem-cell transplantation, indicating that novel strategies are required to improve the survival of patients with relapsed/refractory MM.

In recent years, chimeric antigen receptor (CAR)T-cell immunotherapy, based on the infusion of autologous T cells genetically modified to recognize an antigen

## Correspondence:

BEATRIZ MARTIN-ANTONIO  
bmartina@clinic.cat

Received: June 3, 2019.

Accepted: January 3, 2020.

Pre-published: January 9, 2020.

<https://doi.org/10.3324/haematol.2019.228577>

©2021 Ferrata Storti Foundation

Material published in *Haematologica* is covered by copyright. All rights are reserved to the Ferrata Storti Foundation. Use of published material is allowed under the following terms and conditions:

<https://creativecommons.org/licenses/by-nc/4.0/legalcode>.

Copies of published material are allowed for personal or internal use. Sharing published material for non-commercial purposes is subject to the following conditions:

<https://creativecommons.org/licenses/by-nc/4.0/legalcode>, sect. 3. Reproducing and sharing published material for commercial purposes is not allowed without permission in writing from the publisher.



expressed on the tumor cell, has changed the modality of treatment for certain hematologic malignancies. Specifically, in acute lymphoblastic leukemia and lymphomas targeting CD19 outstanding responses have been achieved from the use of CART cells.<sup>5-8</sup> In MM, B-cell maturation antigen (BCMA)<sup>9-11</sup> has appeared as the most promising target for CART-cell immunotherapy.

Clinical studies in patients with relapsed/refractory MM receiving CART-BCMA cells have documented excellent responses.<sup>12</sup> Unfortunately, however, patients end up relapsing.<sup>12,13</sup> Interestingly, in comparison to CART19, a higher CART-cell dose is required to achieve responses, 150x10<sup>6</sup> CART cells being the lowest dose required to obtain response in patients who have relapsed after or are refractory to a median of seven lines of treatment.<sup>12,14</sup> Moreover, it has been shown that a deepening of the response is obtained over time.<sup>12</sup> In addition, the use of humanized or human CAR instead of murine CAR is emerging as the current trend in CART-cell immunotherapy.<sup>15,16</sup>

Here, using the same structure developed for CAR19 (ARI-0001), a CAR that has already been used in a phase I clinical trial (NCT03144583) for B-cell malignancies at our institution,<sup>17</sup> we generated a murine CAR against BCMA (ARI2m) and a humanized version (ARI2h) for academic use. The efficacy and inflammatory response of both ARI2m and ARI2h cells were compared. Both CART cells showed comparable anti-MM activity. However, a greater efficacy was observed for ARI2h cells in cases of high tumor burden. The feasibility of clinical-grade expansion was tested in parallel in two different institutions and successfully achieved for both CAR. Finally, the impact of soluble BCMA (sBCMA) on ARI2m cell activity was analyzed, demonstrating how sBCMA can negatively affect CAR-BCMA activity. Overall, the results of this study have set the bases for a multicenter clinical trial on the use of ARI2h cells in MM patients in Spain (EudraCT code: 2019-001472-11).

## Methods

### Ethics statement

Research involving human materials was approved by the Clinical Research Ethical Committee (Hospital Clinic, Barcelona, Spain). Peripheral blood T cells were obtained from healthy donors after informed consent. All animal work was performed with approval from the Animal Research Ethical Committee (Hospital Clínic, Barcelona, Spain).

### Cloning and humanization strategy

The anti-BCMA single chain variant fragment (scFv) was designed from the J22.9 antibody.<sup>18</sup> Human CD8a domains, 4-1BB and CD3 domains were obtained from the CART19 used at our Institution.<sup>17</sup> Anti-CD19 scFv was substituted for the anti-BCMA scFv of the J22.9 antibody. In order to obtain ARI2h, the scFv sequence of the J22.9 antibody was humanized using two predictive models (Blast and Germline). Selected amino acids (excluding complementarity-determining regions and Vernier zone) were substituted for their homologous sequence in humans.

### Predictive *in silico* models

Immunogenicity against MHC-I was predicted with NetMHC-4.0<sup>19,21</sup> as previously described.<sup>15</sup> In detail, binding

affinities of every 9-mer peptides from both scFv that are not encoded by the human genome were evaluated for 12 HLA-I alleles (5 type A and 7 type B) to predict binding affinity. As humanized ARI2h scFv contains human framework regions, only sub-peptides from complementarity-determining regions and Vernier zone were considered. The affinity threshold to select only strong binders was <100 nM. To determine binding affinities, structural models derived for each antibody-BCMA pair were built with M4T<sup>22</sup> using the crystal structure of the J22.9xi-BCMAhuman complex (4ZFO)<sup>18</sup> from the Protein Data Bank<sup>23</sup> as a template. The quality and stereochemistry of the model was assessed using Prosa-II<sup>24</sup> and PROCHECK,<sup>25</sup> respectively. For each structural complex antibody-antigen model a total of 100 minimization trajectories were performed, followed by an estimation of the binding affinity as the energy difference between the complex and its separated components (ddG). Minimization and ddG analysis were carried out with Rosetta Design Suite.<sup>26,27</sup> The quality of the binding affinity model was very high<sup>28</sup> because of the high level of sequence identity between target sequences and the template showing similar protein-protein interfaces (*Online Supplementary Figure S1D*).

### Clinical-grade production of ARI2 cells

Lentiviral particles were produced inside a clean room facility following Good Manufacturing Practice guidelines as previously described.<sup>17</sup> Clinical-grade ARI2h/ARI2m cells were produced using CliniMACS Prodigy (Miltenyi, Biotec) as described elsewhere.<sup>17</sup>

Further details of the methods are provided in the *Online Supplementary Methods*.

## Results

### ARI2m cells demonstrate potent anti-myeloma activity

The ARI2m sequence (*Online Supplementary Figure S1A*) contains the scFv sequence of the anti-BCMA antibody J22.9,<sup>18</sup> which has been shown to be effective against MM,<sup>29</sup> and human CD8a, 4-1BB and CD3 $\zeta$  as hinge, transmembrane, co-stimulatory and signaling domains (Figure 1A). CART-cell transfection efficiencies varied between 30-60% in different experiments. CAR expression was retained after cryopreservation (*Online Supplementary Figure S1B*). The efficacy of ARI2m cells was tested against ARP1 and U266 MM cells by co-culturing T cells and MM cells at an effector:target (E:T) ratio of 1:1 over 4 days. ARI2m cells efficiently eliminated MM cells in comparison to untransduced (UT) T cells (Figure 1B) while no cytotoxicity was observed against a BCMA-negative cell line (K562) demonstrating the specificity of ARI2m cells (Figure 1B). In addition, limiting dilution cytotoxicity assays with E:T ratios from 1:1 to 1:0.125 demonstrated a high efficacy of ARI2m cells at eliminating MM cells at a low E:T ratio at 36 h (Figure 1C), and the effect continued to increase to 72 h (*Online Supplementary Figure S1C*).

The production of pro-inflammatory cytokines by ARI2m cells was analyzed after co-culturing ARI2m cells and MM cells at different E:T ratios, at 24 and 48 h. A high interferon (IFN) $\gamma$  production was observed at 24 h which increased at 48 h (Figure 1D). Some IFN $\gamma$  production was detected for UT T cells, as expected, since UT T cells are activated during *in vitro* expansion. Minimum levels of interleukin (IL)6 were detected at 24 h, with the levels increasing

at 48 h (Figure 1D). Tumor necrosis factor (TNF) $\alpha$  production decreased at 48 h in comparison to that at 24 h, suggesting that TNF $\alpha$  is produced early during CART-cell activation (Figure 1D).

The *in vivo* efficacy of ARI2m cells was analyzed in a murine model in which NSG mice received  $1 \times 10^6$  ARP1 MM cells. Mice were treated 6 days later with either  $10 \times 10^6$  UT cells or  $10 \times 10^6$  T cells containing  $2 \times 10^6$  ARI2m cells

(Figure 1E). ARI2m cells prevented disease progression and performed better than UT T cells (Figure 1E, F). As expected, this translated into increased survival (Figure 1G). Furthermore, analysis of mice tissues at the experimental endpoint showed an absence of MM cells in the bone marrow and spleen (Figure 1H). T cells were mainly in the spleen (Figure 1I), whereas CART cells proliferated mainly in bone marrow, as indicated by a higher percentage of

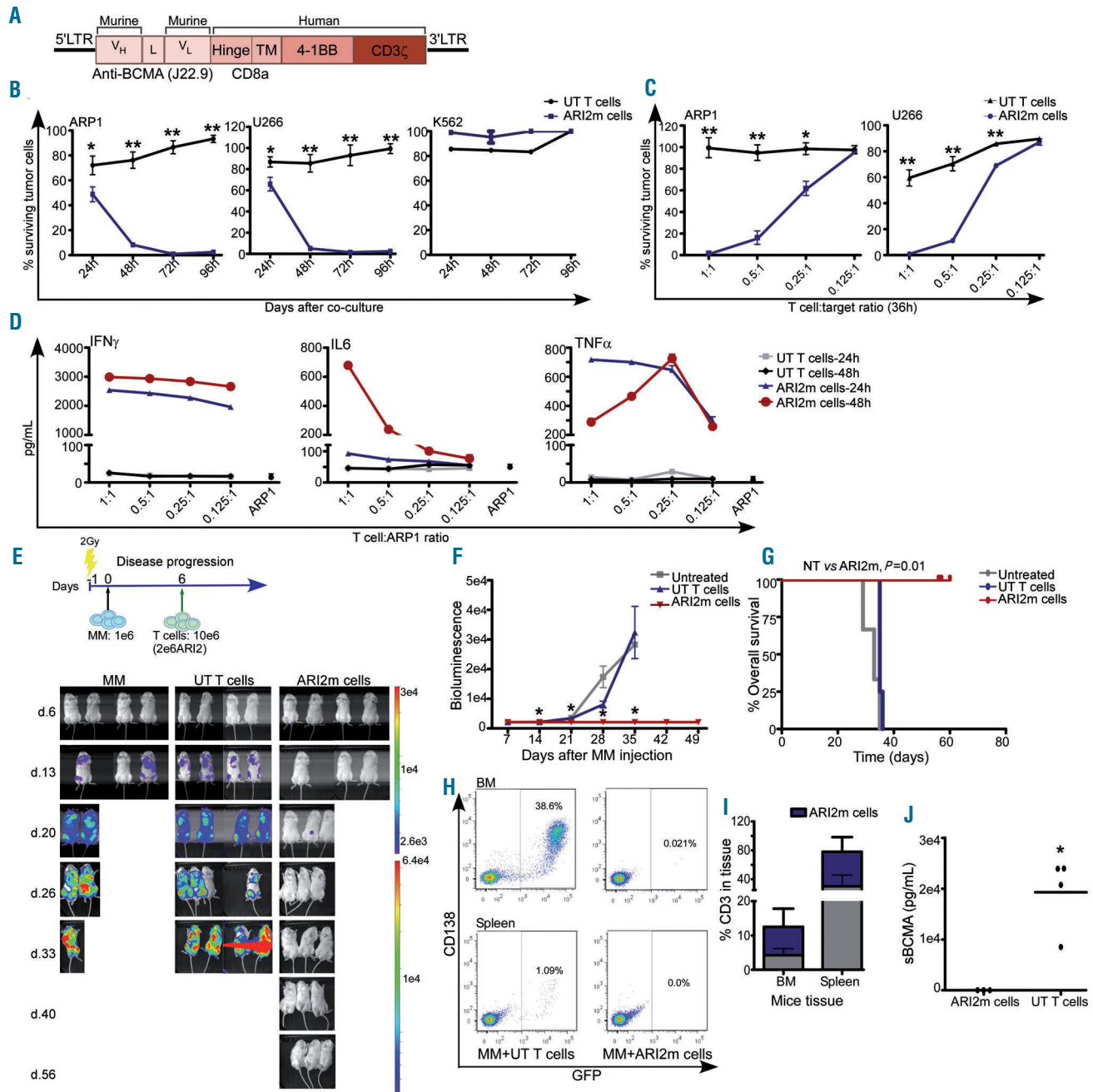


**Figure 1. ARI2m cells demonstrate potent *in vitro* and *in vivo* anti-myeloma activity.** (A) Design of ARI2m. (B) Cytotoxicity assays of ARI2m against ARP1 and U266 (multiple myeloma cell lines) and non-myeloma K562 cells performed from 24–96 h. (C) Limiting dilution cytotoxicity assay against ARP1 and U266 cells performed at ratios from 1:1 to 0.125:1 (T cell: tumor cell line) at 36 h. (D) Cytokine profile of interferon  $\gamma$ , interleukin 6 and tumor necrosis factor  $\alpha$  after 24 h and 48 h of co-culturing T cells and ARP1 cells. (E–J) *In vivo* efficacy of ARI2m cells. (E, F) Diagram of experimental design and quantification of disease progression by weekly bioluminescence imaging and overall survival of the different groups of mice (G). (H) Flow cytometry of bone marrow and spleen of mice at the end of the experiment. (I) Percentage of total T cells and chimeric antigen receptor T cells in bone marrow and spleen of mice treated with ARI2m or UT cells. (J) Soluble B-cell maturation antigen from mice serum after being treated with ARI2m or UT cells. \* $P < 0.05$ . LTR: long terminal repeat; UT: untransduced; IFN $\gamma$ : interferon  $\gamma$ ; IL6: interleukin 6; TNF $\alpha$ : tumor necrosis factor  $\alpha$ ; MM: multiple myeloma; BM: bone marrow; GFP: green fluorescent protein; sBCMA: soluble B-cell maturation antigen.

CART cells from the whole T-cell population in bone marrow than in the spleen (Figure 1I). Moreover, sBCMA was analyzed as an additional marker for MM progression in mice serum. As expected, a high amount of sBCMA was detected in mice treated with UT T cells while no sBCMA was found in mice treated with ARI2m cells (Figure 1J).

### Humanization of ARI2m does not change affinity binding against human B-cell maturation antigen and enhances cytotoxicity against highly advanced myeloma disease

Early disappearance of CART cells<sup>15</sup> is associated with xenorecognition of the murine component of the CAR scFv by the human immune system. To circumvent this problem, we designed a humanized sequence of the scFv of ARI2m (Online Supplementary Figure S1A). Two different humanized variants were created based on two different predictive algorithms (Blast and Germline) by substitution of amino acids of the variable regions of heavy and light chains. *In vitro* comparison of the efficacy of both variants demonstrated that the Germline variant had slightly higher anti-MM activity (Figure 2A) and equal specificity, since neither of them eliminated K562 cells (Figure 2A). Therefore, the Germline variant, which was termed ARI2h, was selected for additional characterization. Predictive *in silico* models for the immunogenicity of both scFv demonstrated higher immunogenicity for ARI2m than for ARI2h (Figure 2B). Binding affinity prediction of both scFv against murine and human BCMA showed that both scFv bind to human BCMA with similar affinity while being unable to bind murine BCMA (Figure 2C). A structural comparison between the two scFv showed that most structural changes during the humanization were concentrated in the heavy chain of the antibody. Complementarity-determining regions on the antibody included no mutations and presented almost no structural drift (Figure 2D), reinforcing the idea that both antibodies have an almost identical binding surface. Subsequently, we analyzed whether T-cell transfection with either ARI2m or ARI2h CAR constructs would lead to different phenotypes in ARI2 cells. We did not observe any difference in either the proportion of ARI2+CD4 and ARI2+CD8 cell populations (Figure 2E) or the proportion of memory T-cell subsets (Online Supplementary Figure S1E).

Moreover, as it was noted that the *in vitro* efficacy of ARI2h was slightly lower than that of ARI2m cells (Figure 2A), a long-term cytotoxicity assay was performed in which tumor and ARI2 cells were cultured together at a low E:T ratio (0.125:1). This assay showed slower killing kinetics for ARI2h cells, but an equal anti-MM activity at later time-points (Figure 2F). Accordingly, T-cell proliferation upon CAR-antigen binding was slower for ARI2h cells (Figure 2G). In addition, whereas the same level of IFN $\gamma$  was produced by both CART cells, lower TNF $\alpha$  and similar IL6 production was detected for ARI2h cells (Figure 2H).

The anti-MM activity of ARI2h and ARI2m cells was further evaluated using two different *in vivo* models of MM (early and advanced disease models). Mice received MM cells on day 0 and were treated with  $5 \times 10^6$  CART cells on day 6 or 14 to create an early and advanced model of disease, respectively (Figure 3A, B). In the early disease model, ARI2h and ARI2m cells prevented MM progression equally (Figure 3A, C). Around day 50, mice started to show signs of toxicity, which were more severe in the ARI2m group and translated into a lower survival rate for this group (Figure 3D). These results suggested that toxicity was related to a

global higher number of T cells proliferating in the ARI2m-treated group, as previously observed.<sup>30</sup> In the advanced disease model, whereas ARI2m abrogated disease progression completely, minimal levels of MM disease were detected in the ARI2h-treated group at certain time points (Figure 3B), although this difference was not statistically significant (Figure 3C). Interestingly, mice treated with ARI2h cells again showed increased survival, consistent with lower toxicity, in comparison with that of mice treated with ARI2m cells (Figure 3D). Accordingly, in both disease models, the global number of T cells was higher for ARI2m than for ARI2h cells (Figure 3E), which might explain the greater xeno-graft-*versus*-host disease observed in the ARI2m-treated group. Importantly, the majority of T cells in bone marrow corresponded to CART cells, for both ARI2m and ARI2h cells, and in both disease models (Figure 3E). Lastly, analysis of mice serum showed that both CAR secreted large amounts of IFN $\gamma$ . However, and in agreement with previous observations of slower kinetics for ARI2h cells, IFN $\gamma$  production was slower in the ARI2h group. Thus, in the early model, IFN $\gamma$  could not be detected in the ARI2h group 3 days after CART-cell infusion but its levels were higher at day 31 (Figure 3F). Similarly, in the advanced disease model, no IFN $\gamma$  was detected at day 5 for ARI2h cells, but levels increased at day 21 (Figure 3F).

These results suggested a faster activity of ARI2m than of ARI2h cells, which in cases of high tumor burden, might lead to faster exhaustion of CART cells and their disappearance. To test this hypothesis, a third *in vivo* experiment with a lower CART-cell dose ( $3 \times 10^6$ ) was performed. Disease burden was higher at the time of CART-cell injection than in the previous experiments (Figure 3B vs. Figure 4A). In this model, neither ARI2m nor ARI2h cells could prevent disease progression (Figure 4B). However, the performance of ARI2h cells at slowing disease progression was better than that of ARI2m cells (Figure 4B). At the last time-point, when mice were euthanized due to disease progression and not to xeno-graft-*versus*-host disease, T cells were almost undetectable (Figure 4C). However, mice treated with ARI2h cells had higher numbers of ARI2h cells in the bone marrow (Figure 4C). These data suggest that slower CART-cell proliferation could lead to longer CART-cell persistence and superior antitumor activity in cases of high tumor burden. To further support these findings, we exposed both ARI2m and ARI2h cells to consecutive *in vitro* challenges with MM (Figure 4D). In agreement with the lower ARI2m efficacy observed in animals with a high tumor burden, these experiments demonstrated more durable persistence for CD4 and CD8 ARI2h cells, which was not consistent for ARI2m cells (Figure 4E).

### ARI2h cells induce less tumor necrosis factor $\alpha$ production than do ARI2m cells

Previous studies have shown that macrophages, after being activated by CART cells, are the main producers of IL6, IL1 $\beta$  and TNF $\alpha$ <sup>31,32</sup> which lead to the development of cytokine release syndrome (CRS) in patients. To further analyze the pro-inflammatory profile of both CAR, we therefore established an *in vitro* system adding macrophages. Thus, effector and target cells were co-culture in the presence of macrophages (Figure 5A). The addition of macrophages did not affect CART-cell cytotoxicity (Figure 5B). The level of IFN $\gamma$  was only slightly increased but very significant increases were detected for IL6, TNF $\alpha$  and IL1 $\beta$ , the last one not being detected in the absence of

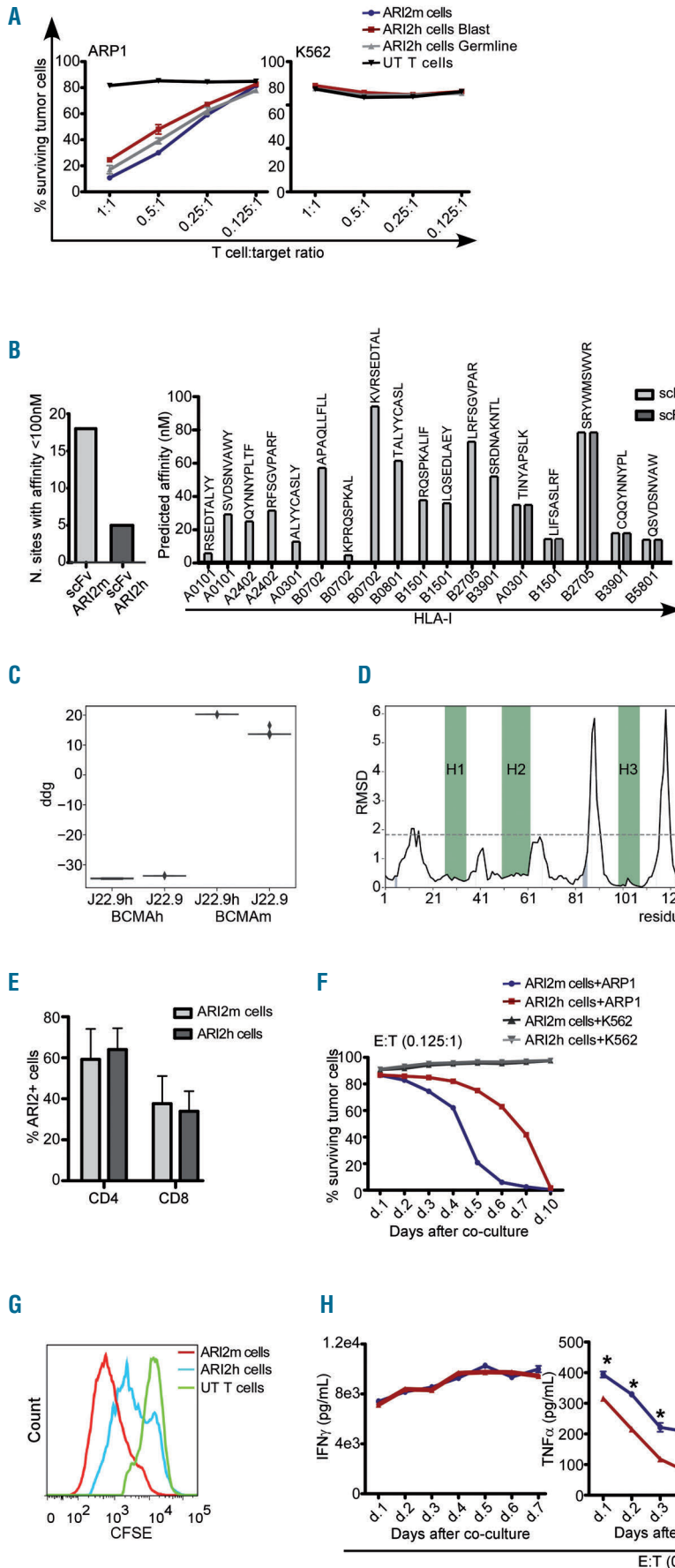


**Figure 2. Humanization of ARI2m into ARI2h and comparison of the affinity and immunogenicity of ARI2m vs ARI2h.** (see also *Online Supplementary Figure S1*). (A) Limiting dilution cytotoxicity assay of ARI2m versus both humanized versions (Blast and Germline). (B) Predicted affinities of 9-mer peptides derived from either the ARI2m or ARI2h single chain variant fragment (scFv) against HLA-I. The total number of sites with predicted affinity <100 nM is shown on the left, and specific interactions of HLA-I alleles with each 9-mer peptide of the scFv is shown on the right. (C) Estimation of the binding affinity of both scFv against human and murine B-cell maturation antigen (BCMA). The difference in Gibbs free energy between the complex and its separated components for each protein pair highlights the inability of any of the antibodies to target murine BCMA. (D). Local structural comparison between the two scFv performed through RMSD. Positions of the complementarity-determining regions are highlighted in green while sequence differences between the two antibodies are mapped in gray under the curve. The resolution of the template structure of the antibody is represented as a dashed line. The graphic shows low structural drift on the antibodies' complementarity-determining regions between the two antibody variants. (E). Phenotype characterization of T cells transduced with either ARI2m or ARI2h chimeric antigen receptor construct and after being expanded for 7 days (n=3). (F) Long-term cytotoxic assay comparing ARI2m versus ARI2h cells against ARP1 (multiple myeloma cells) and K562 (non-myeloma cells) for proliferation (G) and interferon  $\gamma$ , tumor necrosis factor  $\alpha$  and Interleukin 6 production (H). \* $P < 0.05$ . UT: untransduced; ddg: difference in Gibbs free energy; RMSD: root mean square deviation; E:T, effector to target cell ratio; CSFE: carboxyfluorescein succinimidyl ester; IFN $\gamma$ : interferon  $\gamma$ ; TNF $\alpha$ : tumor necrosis factor  $\alpha$ ; IL6: interleukin 6.

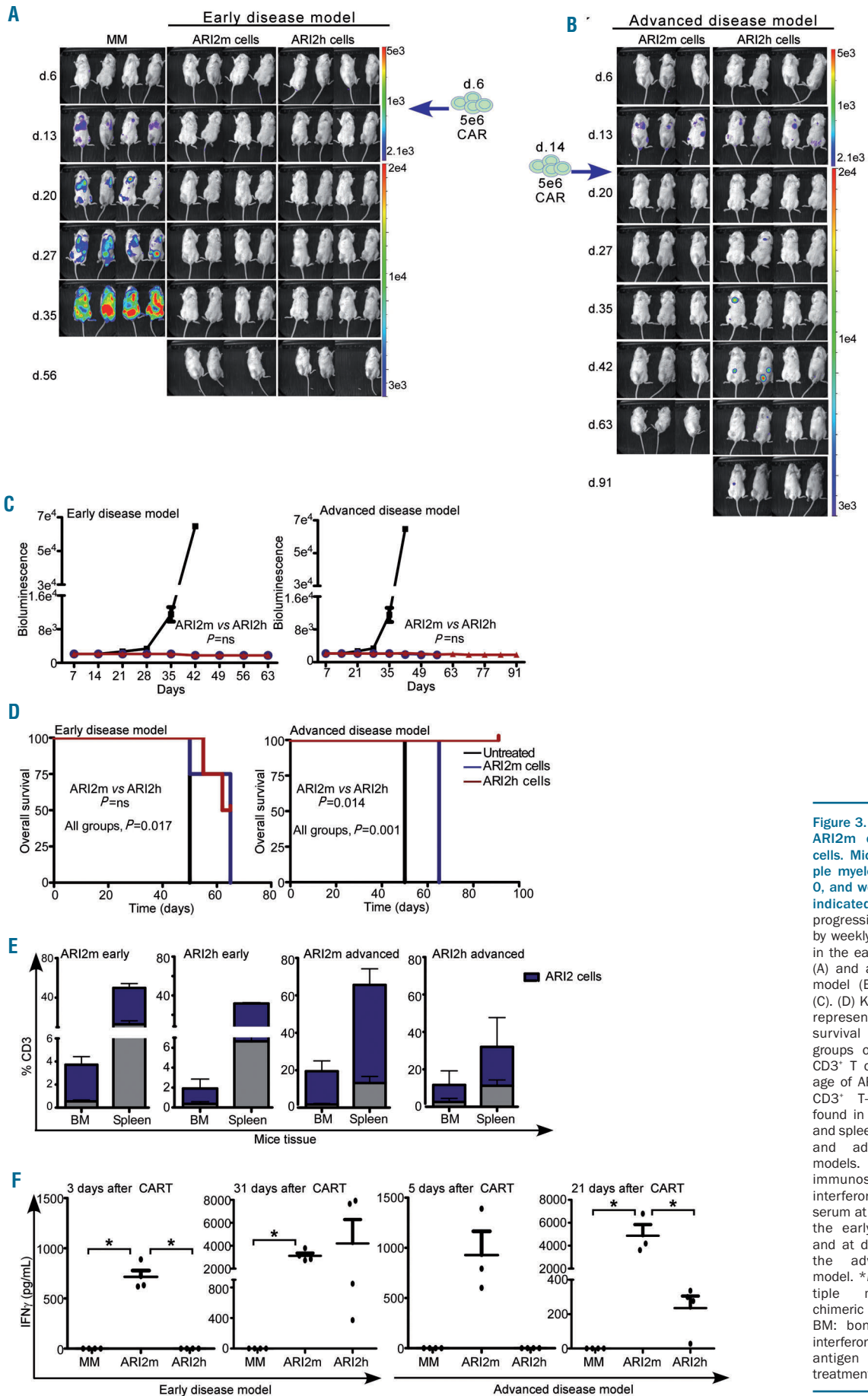


**Figure 3. In vivo efficacy of ARI2m cells and ARI2h cells.** Mice received multiple myeloma cells on day 0, and were treated at the indicated days. Disease progression was followed by weekly bioluminescence in the early disease model (A) and advanced disease model (B) and quantified (C). (D) Kaplan-Meier curve representing the overall survival of the different groups of mice. (E) Total CD3<sup>+</sup> T cells and percentage of ARI2 cells from the CD3<sup>+</sup> T-cell populations found in the bone marrow and spleen in both the early and advanced disease models. (F) Enzyme-linked immunosorbent assay of interferon  $\gamma$  from murine serum at days 3 and 31 for the early disease model and at days 5 and 21 for the advanced disease model. \* $P < 0.05$ . MM: multiple myeloma; CAR: chimeric antigen receptor; BM: bone marrow; IFN $\gamma$ : interferon  $\gamma$ ; CART: chimeric antigen receptor T-cell treatment.

macrophages (Figure 5C). Next, we compared the pro-inflammatory activity of ARI2m cells and ARI2h cells over 2 days using this setting. We observed similar IFN $\gamma$ , IL6 and IL1 $\beta$  production for both CAR (Figure 5D) but TNF $\alpha$  production was lower for ARI2h cells, consistent with the findings of the long-term *in vitro* assay previously performed (Figure 2H) and the lesser *in vivo* toxicity of ARI2h compared to ARI2m cells.

#### Efficient clinical production and activity of ARI2 cells

Pre-clinical data presented here support the development of a phase I multicenter clinical trial for MM patients (EudraCT code: 2019-001472-11) to evaluate the efficacy of treatment with ARI2 cells. The feasibility of large-scale, clinical-grade production was tested both for ARI2m and ARI2h cells using T cells from healthy donors. A CART-cell production system has already been established at our institution and is being used in an ongoing phase I clinical trial with a CAR19 product (ARI-0001).<sup>17</sup> Four expansions were conducted for each CAR in two different institutions. Both

ARI2m and ARI2h cells were efficiently expanded and the required CART-cell dose ( $>150 \times 10^6$  CART cells)<sup>12</sup> was achieved in all cases (Figure 6A, B). Anti-MM activity for both ARI2h and ARI2m cells was also demonstrated (Figure 6C). In both institutions, all productions achieved the minimum threshold required for product release (Figure 6D, E).

#### Soluble and released B-cell maturation antigen affects ARI2 cells activity

Clinical studies with CART19 in acute lymphoblastic leukemia have shown that  $1 \times 10^6$  CART cells/kg are sufficient to achieve complete remission.<sup>5</sup> In MM however a higher dose is needed ( $>150 \times 10^6$ ).<sup>12</sup> BCMA is cleaved and released as sBCMA into the extracellular milieu.<sup>33</sup> We hypothesized that sBCMA can bind to CAR-BCMA, partially hampering its anti-MM activity, thereby explaining the high CAR-BCMA dose required to achieve complete remission in MM patients. We therefore measured the amount of sBCMA in serum from patients with monoclonal gammopathy of undetermined significance, patients with newly

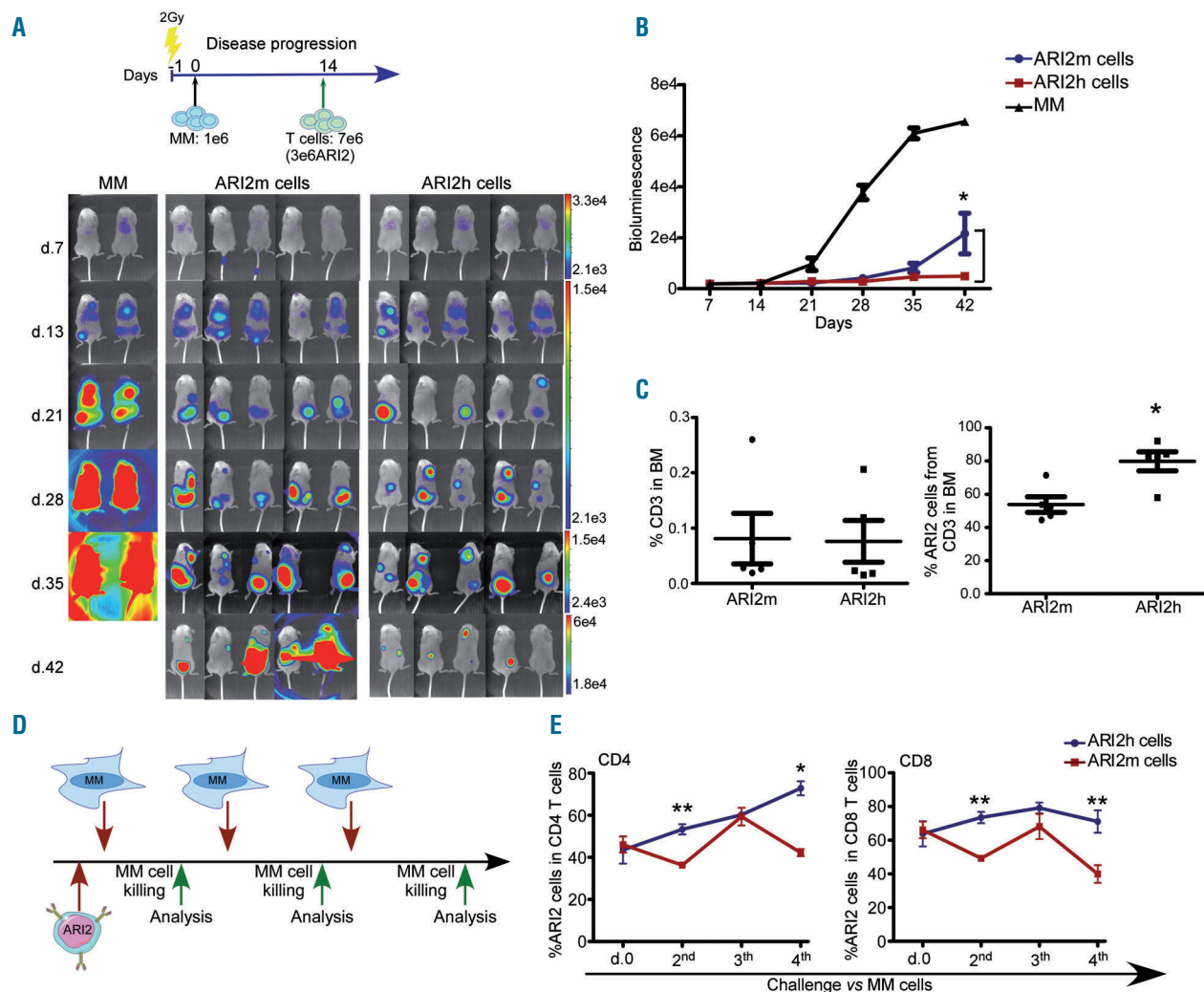


**Figure 4. Humanization of ARI2m enhances cytotoxicity against highly advanced myeloma disease.** (A) Schematic representation and images of an *in vivo* experiment in mice receiving ARP1 multiple myeloma cells (MM) and treated with either ARI2m or ARI2h cells. (B) Disease progression was followed by weekly bioluminescence of the experiment in (A). (C) Total CD3<sup>+</sup> T cells and percentage of ARI2 cells from the CD3<sup>+</sup> T-cell population found in the bone marrow. (D) Graph showing the scheme of consecutive challenges of chimeric antigen receptor T (CAR) cells to MM cells. (E) Percentage of CART cells in CD4 or CD8 T-cell subsets after each challenge. \* $P < 0.05$ . \*\* $P < 0.0001$ .

diagnosed MM and MM patients at relapse. As expected, we observed larger amounts of sBCMA in MM patients (Figure 7A).

To test whether sBCMA inhibits CART-cell activity, MM cells were co-cultured with ARI2m cells in the presence of recombinant BCMA protein. The results confirmed that recombinant BCMA blocks the activity of ARI2m cells, in terms of cytotoxicity and IFN $\gamma$  production (Figure 7B). MM patients had around 100 ng/mL of sBCMA and a titration assay with recombinant BCMA demonstrated inhibition of ARI2m-cell activity up to 32 ng/mL of BCMA (Figure 7C). BCMA shedding is mediated by  $\gamma$ -secretase, which directly cleaves and releases BCMA into the milieu, decreasing surface BCMA expression. BCMA shedding can, therefore, be blocked using  $\gamma$ -secretase inhibitors.<sup>33</sup> To analyze the effect of a  $\gamma$ -secretase inhibitor (DAPT), we measured membrane-bound BCMA in MM cells and the amount of sBCMA before and after treating MM cells with DAPT. As expected, DAPT treatment increased BCMA surface expression in MM cells and decreased the release of sBCMA (Figure 7D, E). The increased membrane-bound BCMA and decreased sBCMA associated with DAPT treatment were also detected after co-culturing MM cells with UT T cells (Figure 7D, E). In the case of co-cultures of ARI2m and MM cells, the addition of DAPT decreased the amount of sBCMA, as expected. However, membrane-bound BCMA was poorly detected because of the high ARI2m-cell activity *in vitro*, eliminating MM cells (Figure 7D, E). Having demonstrated that DAPT treatment prevents BCMA shedding, we tested

whether this effect results in enhanced ARI2m-cell activity. This analysis was conducted in transwell plates, in which untouched MM cells were placed in the upper well and co-cultured ARI2m and MM cells in the lower well (Figure 7F). In this setting, MM cells in the upper well released sBCMA continuously. A cytotoxicity assay showed reduced ARI2m-cell cytotoxicity and IFN $\gamma$  production in the presence of sBCMA (with MM cells in the upper well) than in the control without MM cells in the upper well (Figure 7G). Moreover, the addition of DAPT to this transwell assay enhanced the cytotoxicity and IFN $\gamma$  production of ARI2m cells without affecting the proliferation of ARI2m cells (Figure 7G).

In addition, using confocal fluorescence microscopy we observed that BCMA is released from MM cells in vesicles (Figure 7H) through a mechanism that could also reduce CART-cell activity. In order to confirm that these BCMA vesicles could temporarily affect CAR-BCMA activity, MM cells overexpressing BCMA fused to green fluorescent protein (MM-BCMA-GFP) were co-cultured with ARI2m cells for 3 h and time-lapse *in vivo* imaging was performed. We confirmed that BCMA released in vesicles bind to ARI2m cells, distracting ARI2m cells from their target MM cells (Figure 7I and *Online Supplementary Movie S1*). Moreover, we also observed that, after being in contact with MM cells, ARI2m cells could acquire BCMA in their membranes from the surface of the MM cells and, as a consequence, fratricide was observed between ARI2m cells (Figure 7J and *Online Supplementary Movie S2*). To further confirm this event,

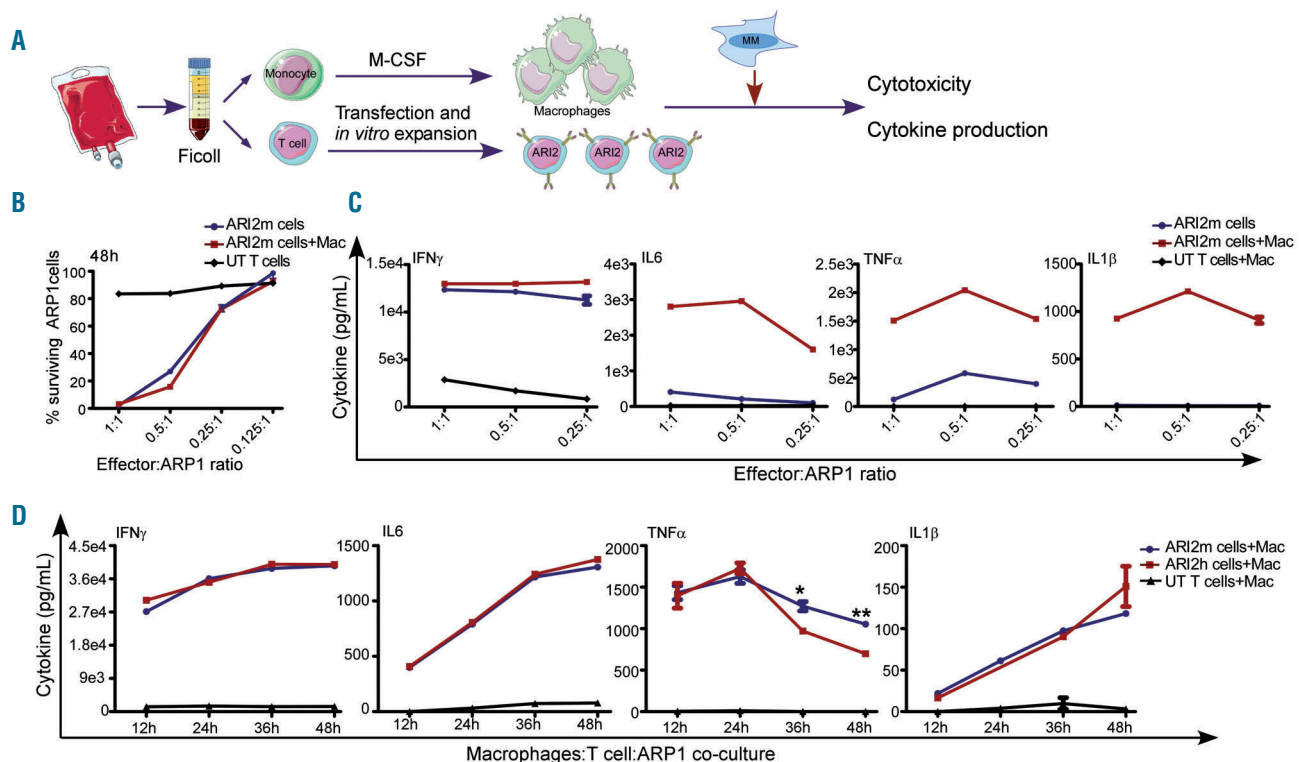


**Figure 5. ARI2h cells induce less tumor necrosis factor  $\alpha$  production than do ARI2m cells.** (A) Schematic representation of monocyte and T-cell isolation from the same buffy coat, differentiation of the monocytes into macrophages, *in vitro* expansion and co-culture of chimeric antigen receptor T (CART) cells with multiple myeloma (MM) cell lines. (B) Cytotoxicity and (C) production of the cytokines interferon  $\gamma$ , interleukin 6, tumor necrosis factor  $\alpha$  and interleukin 1 $\beta$  by ARI2m cells co-cultured with ARP1 cells with or without macrophages. (D) Cytokine production over 48 h after co-culturing ARI2m/ARI2h with macrophages and ARP1 MM cells. Macrophages were added at a 1:3 macrophage:CART ratio. \* $P < 0.05$ . \*\* $P < 0.0001$ . M-CSF: macrophage colony-stimulating factor; UT: untransduced; Mac: macrophages; IFN $\gamma$ : interferon  $\gamma$ ; IL6: interleukin 6; TNF $\alpha$ : tumor necrosis factor  $\alpha$ ; IL1 $\beta$ : interleukin 1 $\beta$ .

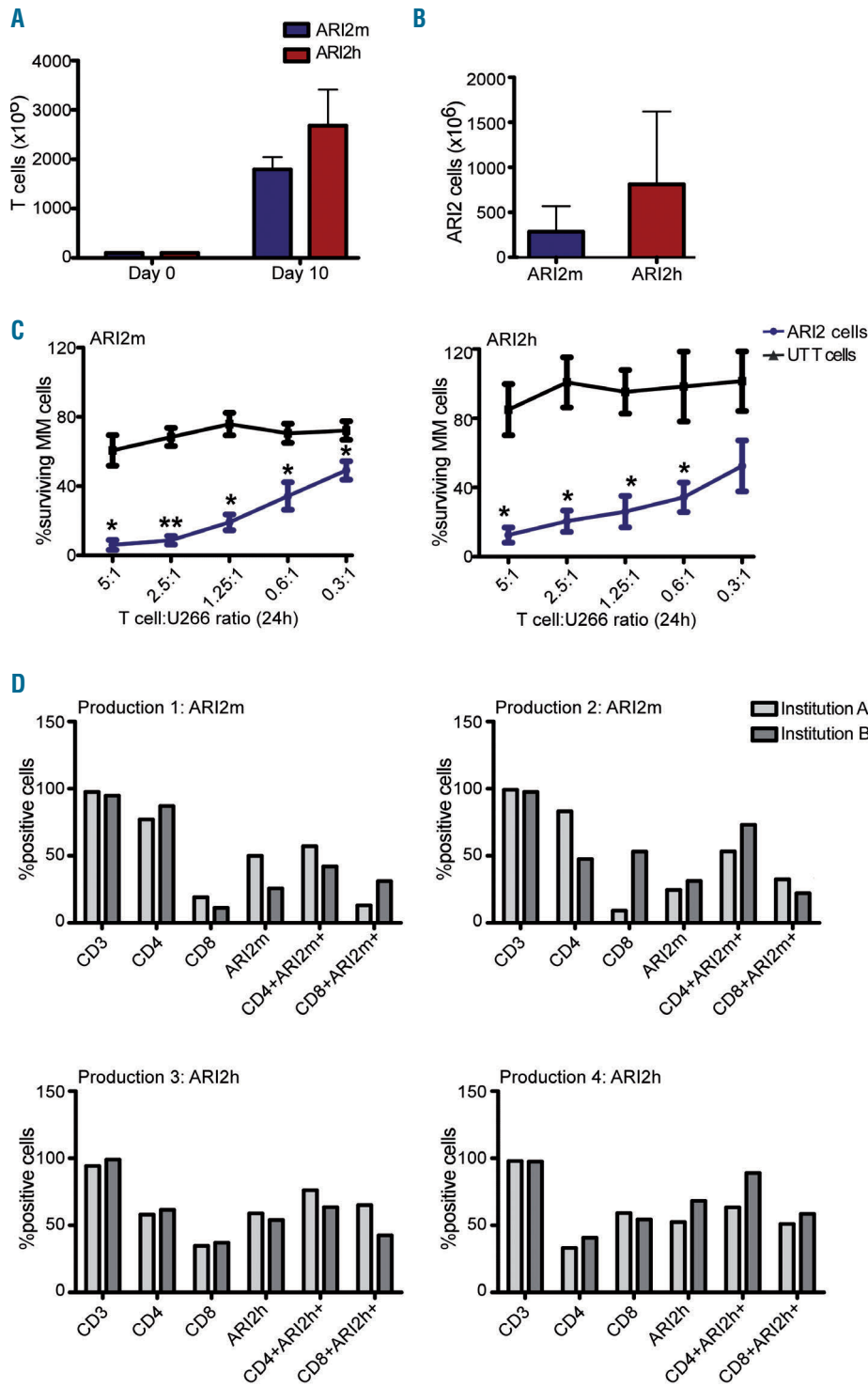


**Figure 6. Efficient clinical production and activities of ARI2m and ARI2h cells.** (A, B) Clinical expansion of ARI2m and ARI2h cells showing the total T-cell (A) and total chimeric antigen receptor T-cell numbers (B) achieved at the end of the expansion. (C) Cytotoxicity assays against the U266 multiple myeloma cell line of both ARI2m and ARI2h cells at the end of the expansion. Results from (A-C) are the median of four clinical expansions of ARI2m and ARI2h cells. (D, E). Detailed comparison of the four clinical productions performed in two different institutions, showing the percentage of each cell population achieved (D) and the specified parameters for product release (E). \* $P < 0.05$ . \*\* $P < 0.0001$ . MM: multiple myeloma; UT: untransduced.

Parameter	Limit	ARI2m (Inst. A)	ARI2m (Inst. A)	ARI2m (Inst. B)	ARI2m (Inst. B)	ARI2h (Inst. A)	ARI2h (Inst. A)	ARI2h (Inst. B)	ARI2h (Inst. B)
Viability	$\geq 70\%$	95%	92%	96%	92.8%	95%	92%	98.7%	89.28%
Sterility	Sterile	Sterile	Sterile	Sterile	Sterile	Sterile	Sterile	Sterile	Sterile
Endotoxins	$\leq 0.5$ UE/mL	<0.5	<0.5	<0.5	<0.5	<0.5	<0.5	<0.5	<0.5
Mycoplasma	Absent	Absent	Absent	Absent	Absent	Absent	Absent	Absent	Absent
N. of integrations	$\leq 10$	7.41	7.3	1.71	1.89	4.56	3.72	0.78	2.95
% ARI2 cells	$> 15\%$	49.9	24.6	25.62	31.21	58.6	52.4	54.08	68.32
Total ARI2 cells	$> 180$ ( $\times 10^6$ )	698	344	625	605	940	1572	2498	1024

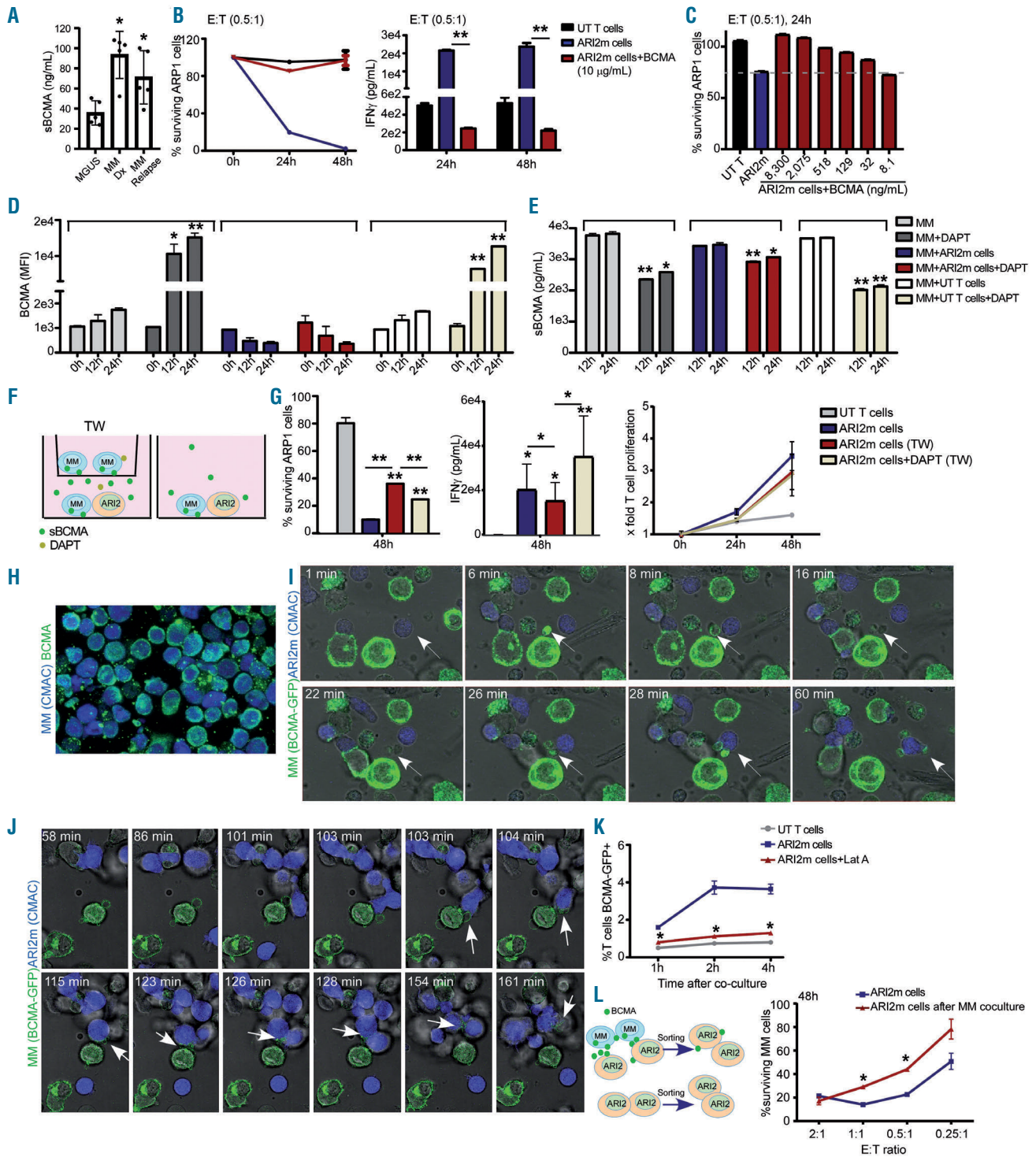


**Figure 7. Soluble and released B-cell maturation antigen affects the activity of ARI2 cells.** (A) Measurement of soluble B-cell maturation antigen (sBCMA) from patients with monoclonal gammopathy of undetermined significance, multiple myeloma (MM) at diagnosis and MM at relapse. (B) Cytotoxicity assay and interferon  $\gamma$  production of ARI2m cells co-cultured with ARP1 MM cells, adding recombinant BCMA protein (BCMA) at 10,000 ng/mL. (C) Cytotoxicity assays (at 24 h) of ARI2m MM cells alone or in co-culture with either ARI2m or UT T cells with or without DAPT. (D, E) Mean fluorescence intensity of BCMA (D) and concentration of sBCMA (E) of ARI2m MM cells alone or in co-culture with either ARI2m or UT T cells with or without DAPT. (F) Design of the cytotoxic assays in transwell plates to analyze the impact of sBCMA and DAPT. ARI2m cells and ARP1 cells were co-cultured in the well, and additional ARP1 cells were added to the transwells as a source of continuous release of sBCMA. (G) Cytotoxicity, interferon  $\gamma$  production and T-cell proliferation in the experiment described in (F). (H) Confocal fluorescence image of MM cells stained with a cell tracker, CMAC, in which BCMA is visualized with a monoclonal anti-BCMA. (I, J) Time lapse images from two different *in vivo* time lapse experiments over 3 h of ARI2m cells stained with the cell tracker, CMAC, and co-cultured with either RPMI MM cells (I) or ARI2m cells (J) overexpressing BCMA in green fluorescent protein (GFP) (see also *Online Supplementary Movies S1* and *S2*). (K) Co-culture assay of T cells with MM-RPMI cells overexpressing BCMA-GFP to which latrunculin A was added in parallel. Percentage of T cells acquiring BCMA-GFP on their surface is shown. (L) MM-RPMI cells and ARI2m cells were co-cultured for 2 h to allow transfer of BCMA-GFP to ARI2m cells, then ARI2m cells were sorted and added into a 48 h cytotoxicity assay against RPMI-MM cells. \* $P < 0.05$ . \*\* $P < 0.0001$ . MGUS: monoclonal gammopathy of undetermined significance; Dx: diagnosis; E:T: effector:target cell ratio; IFN $\gamma$ : interferon  $\gamma$ ; UT: untransduced; MFI: mean fluorescence intensity; DAPT; a  $\gamma$ -secretase inhibitor; TW: transwell; LatA: latrunculin A.

ARI2m and MM cells co-cultured in the presence of a trogocytosis inhibitor (latrunculin A) showed a decreased percentage of BCMA acquisition by ARI2m cells (Figure 7K). In addition, after acquiring BCMA in their membranes, ARI2m cells showed decreased anti-MM activity (Figure 7L).

## Discussion

BCMA was identified in 2013<sup>10</sup> as the most promising antigen for CART-cell immunotherapy for the treatment of patients with relapsed/refractory MM, a finding which was confirmed in different clinical studies in MM patients<sup>12,13</sup> and led us to develop our murine CAR-BCMA cells with 4-1BB as a co-stimulatory domain (ARI2m cells). ARI2m cells demonstrated strong anti-MM activity which is retained in their humanized version (ARI2h cells). Additionally, a greater efficacy of ARI2h *versus* ARI2m cells was observed *in vivo* in mice with high tumor burden. Our results set the bases for a multicenter phase I/II clinical trial of treatment with ARI2h cells for patients with relapsed/refractory MM in Spain.

The success of BCMA as a target for CART-cell immunotherapy was demonstrated for the first time in patients with a CAR-BCMA with CD28 as the co-stimulatory domain. However, this CAR displayed marked toxicity.<sup>14</sup> The CD28 was therefore replaced by 4-1BB: the new CAR (bb2121) demonstrated manageable toxicity and it was found that a minimum dose of 150x10<sup>6</sup> CART cells was required to obtain responses.<sup>12</sup> In parallel, two other studies,<sup>13,34</sup> demonstrated that a lower number of previous treatments is associated with better responses, and that short-term CART-cell expansion is more consistent after lymphodepletion.<sup>34</sup> Different factors influence CART-cell expansion and persistence, which enhance the long-term control of the disease.<sup>5,12,13,34</sup> Work needs to be done to improve these aspects of CAR-BCMA therapy, because a high number of MM patients end up relapsing.<sup>12,13</sup> One of the suggested reasons for this is the limited persistence of CART cells. In this regard, human or humanized CAR, by avoiding the immunological reaction of the human immune system against the murine components of the scFv of the CAR, might increase the persistence of CART cells.<sup>15,16,30</sup> Based on previous studies, and supported by our results showing that both ARI2m and ARI2h cells prevented disease progression equally, we selected ARI2h cells, which are humanized CAR-BCMA cells, to be used for a clinical trial for MM patients (EudraCT code: 2019-001472-11).

Long-term CART-cell persistence is also associated with durability of remission.<sup>5,12,13,34</sup> Factors influencing long-term CART-cell persistence include the exhaustion profile of CART cells<sup>29,35</sup> and the affinity for the target antigen in combination with the co-stimulatory domain of CART cells. In this regard, studies on CART19 with CD28 and 4-1BB demonstrated that strong activation of CART cells, due to high affinity or high expression of the target antigen combined with the CD28 domain, leads to faster CART-cell proliferation with increased exhaustion and shorter persistence. Contrariwise, slower CART-cell activation, due to a lower affinity to the target antigen or to the 4-1BB domain, reduces exhaustion, thereby improving persistence.<sup>35,39</sup> Here, even though ARI2m and ARI2h cells had the 4-1BB co-stimulatory domain and presented the same affinity against human BCMA, ARI2h cells had slower kinetic activity, and demonstrated greater efficacy than ARI2m cells in a murine model

of high tumor burden, and longer persistence after consecutive challenges to tumor cells.

CRS and neurotoxicity are common after the administration of CART cells.<sup>5,12,13,34,40-42</sup> Although these problems are efficiently managed by following international guidelines,<sup>43,44</sup> the ideal CART-cell treatment should try to minimize the development of CRS. Here, the use of ARI2h cells instead of ARI2m was further supported by the observation of lower TNF $\alpha$  production *in vitro* with the ARI2h cells. Whereas IL6 is the effector cytokine for CRS,<sup>31,45,46</sup> and exponentially increases as CRS develops, other cytokines such as TNF $\alpha$  and IL1 $\beta$ <sup>31,32</sup> are the main initiators of CRS, as they are produced at early time points by monocytes and macrophages once they are activated by IFN $\gamma$  produced by CART cells. In fact, TNF $\alpha$ , acts as an initiator cytokine orchestrating the cytokine cascade in many inflammatory diseases, appearing as a therapeutic target in inflammatory diseases.<sup>46</sup> Here, our *in vitro* model with macrophages mimicking a model more similar to the *in vivo* scenario, demonstrated that ARI2h cells induced less TNF $\alpha$  production by macrophages, a relevant finding, as CRS in MM patients after CAR-BCMA treatment associates with a higher peak of TNF $\alpha$ .<sup>12</sup> Moreover, CAR with faster kinetics associate with higher CRS,<sup>37</sup> suggesting that the slower kinetics of ARI2h cells in comparison to ARI2m cells might also explain the observed lower level of *in vivo* toxicity.

Last, we analyzed the impact of sBCMA on CART-cell activity. Even though studies with CAR-BCMA in MM have not found any correlation between sBCMA and CART-cell activity,<sup>10,12,34,47</sup> we observed that the high *in vitro* CART activity rapidly eliminating MM cells impeded a proper analysis of the role of sBCMA in preclinical studies. Our *in vitro* models performed at a low CAR-BCMA:MM ratio, with the creation of an environment with continuous release of sBCMA, and the addition of a  $\gamma$ -secretase inhibitor confirmed the negative impact of sBCMA on CAR-BCMA activity. Moreover, we observed that BCMA is also released in vesicle structures, distracting CART cells from their targets, and that BCMA can be transferred to CART cells through a mechanism which appears to be trogocytosis, a finding already made for CART19 cells,<sup>48</sup> causing decreased anti-MM activity of the ARI2m cells.

In conclusion, we have developed CAR-BCMA cells with 4-1BB as a co-stimulatory domain which have been humanized, retaining high efficacy and demonstrating less toxicity than their murine counterparts. ARI2 cells can be efficiently expanded under Good Manufacturing Practice conditions for use in a clinical trial. Moreover, we demonstrated that sBCMA and BCMA released from MM cells can affect CART-cell activity.

## Disclosures

No conflicts of interests to disclose.

## Contributions

LPA and BMA designed the study, LPA performed *in vitro* and *in vivo* experiments. GS performed clonings, virus production and *in vivo* experiments. LPA and BMA analyzed data and wrote the manuscript. AN designed the scFv of ARI2m and provided viral vector for GFP-Ffluc. MC and AA provided advice for experiments. AA performed some of the CART *in vitro* expansions. MJ, SI and AL performed clinical grade ARI2 production. JB and NFF performed predictive models for binding affinity. CB performed cell sortings. AUI provided funding and constructive ideas. All authors reviewed the manuscript.

### Acknowledgments

We acknowledge the Multiple Myeloma Research Center (Little Rock, AK, USA) for providing the ARP1 cell line and the Confocal Fluorescence Microscopy facilities at the University of Barcelona.

### Funding

Celgene and the Carlos III Institute of Health (project: PI17/01043) provided funding for all in vitro and in vivo studies.

### References

- Palumbo A, Anderson K. Multiple myeloma. *N Engl J Med*. 2011;364(11):1046-1060.
- Kumar SK, Callander NS, Alsina M, et al. Multiple myeloma, version 3.2017, NCCN clinical practice guidelines in oncology. *J Natl Compr Canc Netw*. 2017;15(2):230-269.
- Cancer Stat Facts: Myeloma. National Cancer Institute Surveillance, Epidemiology, and End Results Program Web site. Available at <http://seercancer.gov/statfacts/html/mulmyhtml>. [Accessed January 2, 2020]
- Martinez-Lopez J, Blade J, Mateos MV, et al. Long-term prognostic significance of response in multiple myeloma after stem cell transplantation. *Blood*. 2011;118(3):529-534.
- Maude SL, Laetsch TW, Buechner J, et al. Tisagenlecleucel in children and young adults with B-cell lymphoblastic leukemia. *N Engl J Med*. 2018;378(5):439-448.
- Schuster SJ, Svoboda J, Chong EA, et al. Chimeric antigen receptor T cells in refractory B-cell lymphomas. *N Engl J Med*. 2017;377(26):2545-2554.
- Park JH, Riviere I, Gonen M, et al. Long-term follow-up of CD19 CAR therapy in acute lymphoblastic leukemia. *N Engl J Med*. 2018;378(5):449-459.
- Neelapu SS, Locke FL, Bartlett NL, et al. Axicabtagene ciloleucel CAR T-cell therapy in refractory large B-cell lymphoma. *N Engl J Med*. 2017;377(26):2531-2544.
- O'Connor BF, Raman VS, Erickson LD, et al. BCMA is essential for the survival of long-lived bone marrow plasma cells. *J Exp Med*. 2004;199(1):91-98.
- Carpenter RO, Evbuomwan MO, Pittaluga S, et al. B-cell maturation antigen is a promising target for adoptive T-cell therapy of multiple myeloma. *Clin Cancer Res*. 2013;19(8):2048-2060.
- Novak AJ, Darce JR, Arendt BK, et al. Expression of BCMA, TACI, and BAFF-R in multiple myeloma: a mechanism for growth and survival. *Blood*. 2004;103(2):689-694.
- Raje N, Berdeja J, Lin Y, et al. Anti-BCMA CAR T-cell therapy bb2121 in relapsed or refractory multiple myeloma. *N Engl J Med*. 2019;380(18):1726-1737.
- Zhao WH, Liu J, Wang BY, et al. A phase 1, open-label study of LCAR-B38M, a chimeric antigen receptor T cell therapy directed against B cell maturation antigen, in patients with relapsed or refractory multiple myeloma. *J Hematol Oncol*. 2018;11(1):141.
- Ali SA, Shi V, Maric I, et al. T cells expressing an anti-B-cell maturation antigen chimeric antigen receptor cause remissions of multiple myeloma. *Blood*. 2016;128(13):1688-1700.
- Sommermeier D, Hill T, Shamah SM, et al. Fully human CD19-specific chimeric antigen receptors for T-cell therapy. *Leukemia*. 2017;31(10):2191-2199.
- Turtle CJ, Hanafi LA, Berger C, et al. CD19 CAR-T cells of defined CD4+CD8+ composition in adult B cell ALL patients. *J Clin Invest*. 2016;126(6):2123-2138.
- Castella M, Boronat A, Martin-Ibanez R, et al. Development of a novel anti-CD19 chimeric antigen receptor: a paradigm for an affordable CAR T cell production at academic institutions. *Mol Ther Methods Clin Dev*. 2018;12:134-144.
- Oden F, Marino SF, Brand J, et al. Potent anti-tumor response by targeting B cell maturation antigen (BCMA) in a mouse model of multiple myeloma. *Mol Oncol*. 2015;9(7):1348-1358.
- Lundegaard C, Lamberth K, Hamdahl M, Buus S, Lund O, Nielsen M. NetMHC-3.0: accurate web accessible predictions of human, mouse and monkey MHC class I affinities for peptides of length 8-11. *Nucleic Acids Res*. 2008;36(Web Server issue):W509-512.
- Andreatta M, Nielsen M. Gapped sequence alignment using artificial neural networks: application to the MHC class I system. *Bioinformatics*. 2016;32(4):511-517.
- Nielsen M, Andreatta M. NetMHCpan-3.0; improved prediction of binding to MHC class I molecules integrating information from multiple receptor and peptide length datasets. *Genome Med*. 2016;8(1):33.
- Fernandez-Fuentes N, Madrid-Aliste CJ, Rai BK, Fajardo JE, Fiser A. M4T: a comparative protein structure modeling server. *Nucleic Acids Res*. 2007;35(Web Server issue):W363-368.
- Berman HM, Westbrook J, Feng Z, et al. The protein data bank. *Nucleic Acids Res*. 2000;28(1):235-242.
- Sippl MJ. Recognition of errors in three-dimensional structures of proteins. *Proteins*. 1993;17(4):355.
- Laskowski RA, MacArthur MW, Moss DS, Thornton J. PROCHECK: a program to check the stereochemical quality of protein structures. *J Appl Cryst*. 1993;26:283-291.
- Fleishman SJ, Leaver-Fay A, Corn JE, et al. RosettaScripts: a scripting language interface to the Rosetta macromolecular modeling suite. *PLoS One*. 2011;6(6):e20161.
- Leaver-Fay A, Tyka M, Lewis SM, et al. ROSETTA3: an object-oriented software suite for the simulation and design of macromolecules. *Methods Enzymol*. 2011;487:545-574.
- Baker D, Sali A. Protein structure prediction and structural genomics. *Science*. 2001;294(5540):93-96.
- Bluhm J, Kieback E, Marino SF, et al. CAR T cells with enhanced sensitivity to B cell maturation antigen for the targeting of B cell non-Hodgkin's lymphoma and multiple myeloma. *Mol Ther*. 2018;26(8):1906-1920.
- Smith EL, Staehr M, Masakayan R, et al. Development and evaluation of an optimal human single-chain variable fragment-derived BCMA-targeted CAR T cell vector. *Mol Ther*. 2018;26(6):1447-1456.
- Giavridis T, van der Stegen SJC, Eyquem J, Hamieh M, Piersigilli A, Sadelain M. CAR T cell-induced cytokine release syndrome is mediated by macrophages and abated by IL-1 blockade. *Nat Med*. 2018;24(6):731-738.
- Norelli M, Camisa B, Barbiera G, et al. Monocyte-derived IL-1 and IL-6 are differentially required for cytokine-release syndrome and neurotoxicity due to CAR T cells. *Nat Med*. 2018;24(6):739-748.
- Laurent SA, Hoffmann FS, Kuhn PH, et al.  $\gamma$ -Secretase directly sheds the survival receptor BCMA from plasma cells. *Nat Commun*. 2015;6:7333.
- Cohen AD, Garfall AL, Stadtmauer EA, et al. B cell maturation antigen-specific CAR T cells are clinically active in multiple myeloma. *J Clin Invest*. 2019;129(6):2210-2221.
- Salter AI, Ivey RG, Kennedy JJ, et al. Phosphoproteomic analysis of chimeric antigen receptor signaling reveals kinetic and quantitative differences that affect cell function. *Sci Signal*. 2018;11(544).
- Long AH, Haso WM, Sterm JF, et al. 4-1BB costimulation ameliorates T cell exhaustion induced by tonic signaling of chimeric antigen receptors. *Nat Med*. 2015;21(6):581-590.
- Milone MC, Fish JD, Carpenito C, et al. Chimeric receptors containing CD137 signal transduction domains mediate enhanced survival of T cells and increased antileukemic efficacy in vivo. *Mol Ther*. 2009;17(8):1453-1464.
- Wherry EJ, Kurachi M. Molecular and cellular insights into T cell exhaustion. *Nat Rev Immunol*. 2015;15(8):486-499.
- Smith-Garvin JE, Koretzky GA, Jordan MS. T cell activation. *Ann Rev Immunol*. 2009;27:591-619.
- Schuster SJ, Svoboda J, Chong EA, et al. Chimeric antigen receptor T cells in refractory B-cell lymphomas. *N Engl J Med*. 2017;377(26):2545-2554.
- Locke FL, Neelapu SS, Bartlett NL, et al. Phase 1 results of ZUMA-1: a multicenter study of KTE-C19 anti-CD19 CAR T cell therapy in refractory aggressive lymphoma. *Mol Ther*. 2017;25(1):285-295.
- Shah N, Alsina M, Siegel DS, et al. Initial results from a phase 1 clinical study of bb21217, a next-generation anti-BCMA CAR T therapy. *Blood*. 2018;132(Suppl 1):488.
- Porter D, Frey N, Wood PA, Weng Y, Grupp SA. Grading of cytokine release syndrome associated with the CAR T cell therapy tisagenlecleucel. *J Hematol Oncol*. 2018;11(1):35.
- Lee DW, Santomasso BD, Locke FL, et al. ASTCT consensus grading for cytokine release syndrome and neurologic toxicity associated with immune effector cells. *Biol Blood Marrow Transplant*. 2019;25(4):625-638.
- Hunter CA, Jones SA. IL-6 as a keystone cytokine in health and disease. *Nat Immunol*. 2015;16(5):448-457.
- Parameswaran N, Patil S. Tumor necrosis factor- $\alpha$  signaling in macrophages. *Crit Rev Eukaryot Gene Expr*. 2010;20(2):87-103.
- Friedman KM, Garrett TE, Evans JW, et al. Effective targeting of multiple B-cell maturation antigen-expressing hematological malignancies by anti-B-cell maturation antigen chimeric antigen receptor T Cells. *Hum Gene Ther*. 2018;29(5):585-601.
- Hamieh M, Dobrin A, Cabriolu A, et al. CAR T cell trogocytosis and cooperative killing regulate tumour antigen escape. *Nature*. 2019;568(7750):112-116.